Implementation and Experimental Results of a Three-Transmitter Three-Receiver OFDM/BLAST Testbed

Weidong Xiang, University of Michigan, Dearborn; Deric Waters, Thomas G. Pratt, John Barry, and Brett Walkenhorst, Georgia Institute of Technology

ABSTRACT

A three-transmitter three-receiver orthogonal frequency-division multiplexing Bell Laboratories layered space-time testbed is set up, which achieves a peak data rate of 281.25 Mb/s and a spectral efficiency of 14.4 b/Hz/s. The transmitter of the testbed consists of three signal generators transmitting three independent OFDM signals at 25 Msamples/s synchronously. Three synchronized receiving links are used, each of which includes an RF receiver, an analog-to-digital converter, a digital downconverter, and a PowerPC processor for baseband processing. The performance and complexity of three typical BLAST detection techniques (linear detection, ordered decision feedback detection, and partial decision detection) are evaluated and compared using the data from the experiments conducted in both line-of-sight and non-line-of-sight indoor environments.

INTRODUCTION

Spectrum is an increasingly valuable commodity today, and researchers have been grappling with approaches to achieve high-speed transmission in spite of constraints imposed by limited bandwidth allowances.

In the past, wireless communications links have primarily been single-input single-output (SISO) systems. For these systems, the unavoidable and uncontrollable impairment resulting from multipath propagation is usually regarded as an impediment to high-speed data transmission. In the presence of multipath propagation, the receiver captures several delayed versions of the transmitted signals. The delay spread of the multipath signals, if sufficiently large, results in frequency-selective fading, which in turn limits the maximum data rate that can be transmitted through the channel without introducing intersymbol interference (ISI).

In an endeavor to find ways of improving spectral efficiency, researchers are now focusing attention on multiple-input multiple-output (MIMO) systems, which are capable of realizing spectral efficiencies that far exceed those of SISO systems. Bell Laboratories layered space-time (BLAST), one of the commonly used MIMO architectures, transmits independent data streams in parallel at the same frequency. Although the signals are co-channel and time-coincident, the receiver can still separate the data streams using the array of received signals if it has at least as many antennas as the transmitter and knows the channel properties. The BLAST scheme can increase capacity by a factor of the minimum of the number of transmit antennas and the number of receive antennas. For an 8×12 narrowband MIMO system, spectral efficiencies between 20–40 b/Hz/s have been reported in a typical indoor environment, which are much larger than those of SISO systems [1].

A complementary modulation technique known as orthogonal frequency-division multiplexing (OFDM) has emerged as an efficient method to transfer high-speed data through dispersive channels. It delivers information in parallel over M subcarriers, where M is the fast Fourier transform (FFT) block size. Each subcarrier has a bandwidth equal to $1/M$ of the total signal bandwidth and experiences a flat fading channel. By inserting a cyclic prefix (CP) in front of an OFDM symbol, ISI is virtually eliminated if the maximum channel delay spread is less than the time duration of the CP.

The IEEE 802.16 standard is designed to provide wireless broadband access for metropolitan area networks (MANs). This technology provides a flexible low-cost infrastructure compared to widely deployed Ethernet and digital subscriber line (DSL) networks [2].

In order to demonstrate recent advances in the area of high-speed wireless communications, researchers in the Software Radio Laboratory at the Georgia Institute of Technology implemented a three-transmitter three-receiver (3×3) OFDM/BLAST testbed based on the IEEE

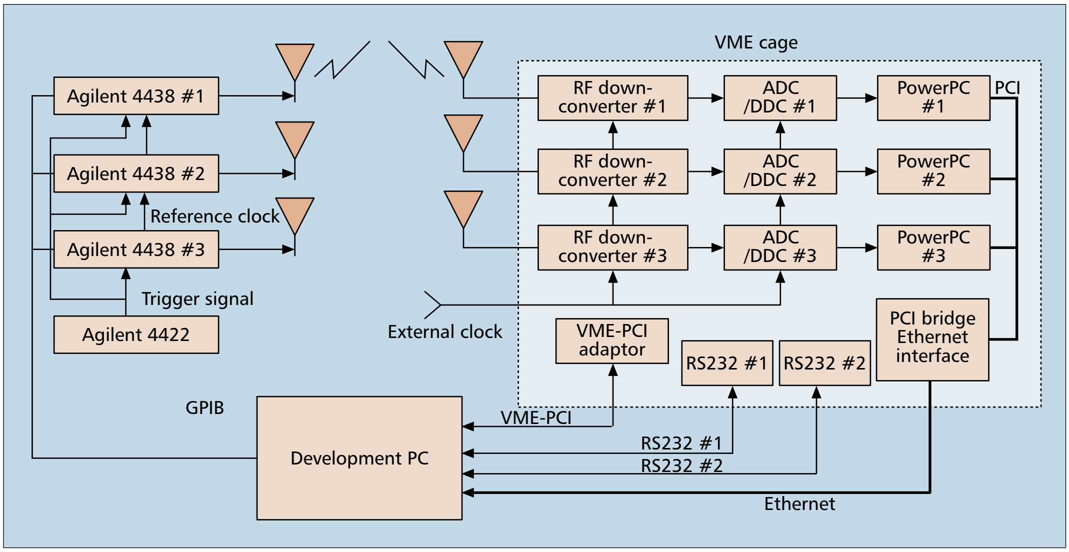

Figure 1. *A block diagram of the 3 × 3 OFDM/BLAST wireless MAN testbed.*

The spurious-free dynamic range (SFDR), defined as the ratio of the root mean square amplitude of the signal to that of the peak of the spurious spectral components including harmonics, is around 80 dBc. The 100 MHz sample clock allows the receiver to over-sample the received signal by four times.

802.16 standard. In a typical indoor environment, the testbed achieved a peak data rate of 281.25 Mb/s with a bit error rate (BER) close to 10^{-5} at a signal-to-noise ratio (SNR) of 35 dB. This data rate nearly triples the 100 Mb/s of commonly used Ethernet connections. Although a few OFDM/BLAST testbeds have been reported recently [1, 3–6], few if any have been based on the IEEE 802.16 standard, and the reported data rates have been substantially smaller than the rates reported in this article.

The authors published an article in *IEEE Communications Magazine*, June 2004, presenting a wireless MAN testbed based on the IEEE 802.16 standard and space-time coding technology with a data rate of 30 Mb/s [7]. The testbed is a two-transmitter two-receiver wireless link, where baseband processing was implemented in Texas Instrument's TMS320C6701 digital signal processors (DSPs) in real-time mode. The 3 × 3 OFDM/BLAST testbed reported in this article is a non-real-time wireless link, where data is collected in real time, but baseband processing is performed using Matlab code in an offline mode. This offline processing approach allows us to evaluate the performance of higher data rates.

Configuration of the 3 × 3 OFDM/BLAST Testbed

In this section we describe the configuration of the testbed and some key modules, including the MPC7410 PowerPC processor, analog-to-digital converter (ADC), digital downconverter (DDC), and radio frequency (RF) downconverter.

MPC7410 PowerPC Processor

The MPC7410 is a 32-bit processor manufactured by Motorola. It utilizes a vector engine to perform parallel processing and offers single-cycle double-precision floating-point processing, full symmetric multiprocessing capabilities, and has 2 Mbytes of cache. The processor operates at a clock as high as 400 MHz and provides attractive calculation power. For example, it takes around 6 ms to finish a 256 complex fast Fourier transform (FFT) operation, about four times as fast as the TMS320C6701 DSP.

ADC and DDC

The Analog Devices AD9432 is a 12-bit ADC operating at a 100 MHz clock. It is a multibit pipeline converter with a switched capacitor architecture. An on-chip track-and-hold circuit is employed to ensure a flat dynamic range. The spurious-free dynamic range (SFDR), defined as the ratio of the root mean square amplitude of the signal to that of the peak of the spurious spectral components including harmonics, is around 80 dBc. The 100 MHz sample clock allows the receiver to oversample the received signal by four times.

The GC1012B is an intermediate frequency (IF)-to-baseband DDC followed by a low pass filter with a passband ripple less than 0.2 dB and out-of-band rejection over 75 dB. The internal local oscillator (LO) has a 28-bit accumulator that provides a tuning accuracy of less than 1 Hz. The baseband samples are output in the format of complex or real, packed or unpacked.

RF Downconverter

The RF downconverter is mounted in a standard VersaModule Eurocad (VME) cage. It shifts the RF signal to an IF centered at 16 MHz with 28 MHz bandwidth. The noise figure of the low noise amplifier is about 3.8 dB, and the SFDR of the receive chain is 75 dBc. Two large-scale input and output attenuators are also integrated.

The LO of the RF downconverter uses multiple phase lock loops (PLLs) to generate clocks with a tuning resolution of 1 Hz.

The Transmitter

The transmitter consists of three Agilent ESG4438C signal generators, which work as arbitrary waveform generators. An Agilent ESG4422 signal generator is used to synchronize the other three signal generators, which are phase locked to each other through a 10 MHz

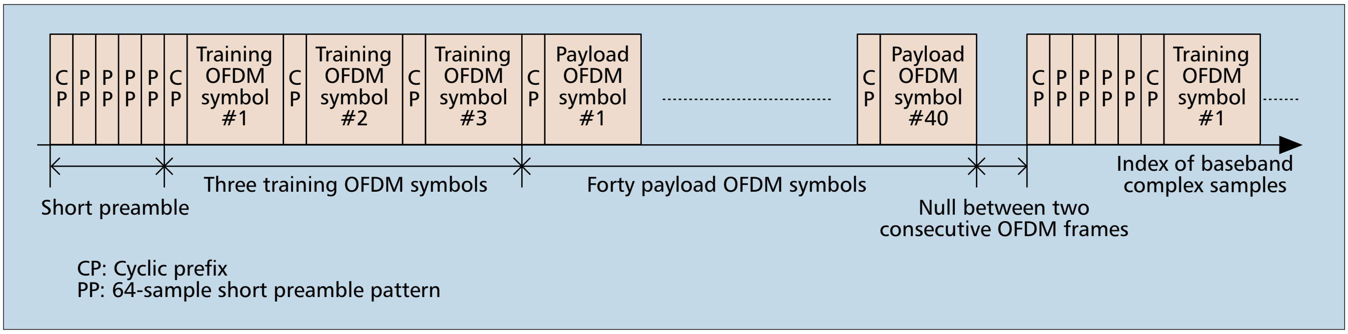

Figure 2. *The construction of the OFDM frame.*

reference clock. The signal generators are connected to a development computer through a general-purpose interface bus (GPIB), as shown in Fig. 1.

Three independent data streams are encoded by Reed-Solomon (RS) encoders, mapped into 64-quadrature amplitude modulation (QAM) symbols, and undergo inverse FFT (IFFT) to form three OFDM frames, shown in Fig. 2. Each OFDM frame consists of a short preamble given by the IEEE 802.16 standard used for time and frequency synchronizations, three training OFDM symbols designed to estimate the channel gains, and forty payload OFDM symbols. Some nulls are inserted between two consecutive OFDM frames.

The three OFDM frames are preloaded to the three signal generators through the GPIB interface. The three signal generators send the synchronous OFDM frames at 25 Msamples/s at a carrier frequency of 2435 MHz. The transmit antennas are omnidirectional and separated by half a wavelength.

The Receiver

The receiver consists of three synchronized receive chains, each of which includes an RF downconverter, an ADC, a DDC, and a PowerPC processor. A VME-peripheral component interconnect (PCI) interface is employed to set the parameters of the RF downconverters. The PowerPC development platform, Tornado, runs in a VxWorks environment set up by two RS-232 interfaces.

First, the three RF converters translate the RF signals to an IF of 16 MHz. Next, the IF signals are sampled at 100 MHz with 12-bit ADCs. The DDCs downconvert the IF signal to complex baseband. As part of the conversion process, the baseband samples are filtered and decimated by a factor of 4 to reduce the sample rate from 100 to 25 Msamples/s.

The three received baseband signals are each passed to the caches of the three PowerPCs via first-in first-out (FIFO) buffers by using direct memory access (DMA) transfers. When the caches are full, the PowerPCs dump the baseband signals to the development computer through an Ethernet interface. 100,000 samples are captured for each baseband signal in each trial. These baseband signals are then handled with a demodulation algorithm that recovers the transmitted data. Given the current system configuration, demodulation of 3 × 3 OFDM/BLAST data is unrealistic for real-time operating at 25 Msamples/s. For the purpose of demonstration, the demodulation processing is done in offline mode.

Table 1 lists the main specifications of the 3 × 3 OFDM/BLAST wireless MAN testbed. The raw data rate is calculated by 25 Mamples/s × 6 b/sample × 3 = 450 Mb/s. This data rate is further reduced because of the overhead in the frequency and time domains. Fifty-six of the 256 subcarriers are zero padded, and the CP takes one-fourth of an OFDM symbol size, so the actual data rate is 450 Mb/s × 200/256 × 256/320 = 281.25 Mb/s. The actual signal bandwidth is 25 MHz × 200/256 = 19.53125 MHz.

Figure 3 illustrates a block diagram of the baseband processing performed at the transmitter and receiver. It includes synchronization, FFT, channel estimation, and BLAST demodulation, which are described in detail. Figures 4 and 5 show the transmitter and receiver of the testbed, respectively.

FFT block size	256
Cyclic prefix	64
OFDM symbol size	320
Number of subcarriers	200
Carrier frequency	2435 MHz
Signal bandwidth	19.53125 MHz
Sample rate	25 Msamples/s
Modulation	64-QAM
Data rate	281.25 Mb/s
Frame preamble	Based on IEEE 802.16 standard
Coding rate	215/255 (RS)

Table 1. *The specifications of the 3 × 3 OFDM/BLAST testbed.*

Initial Baseband Processing at the Receiver

Here we discuss the baseband processing to be performed before the layered data streams are separated. This initial baseband processing includes time synchronization, carrier frequency

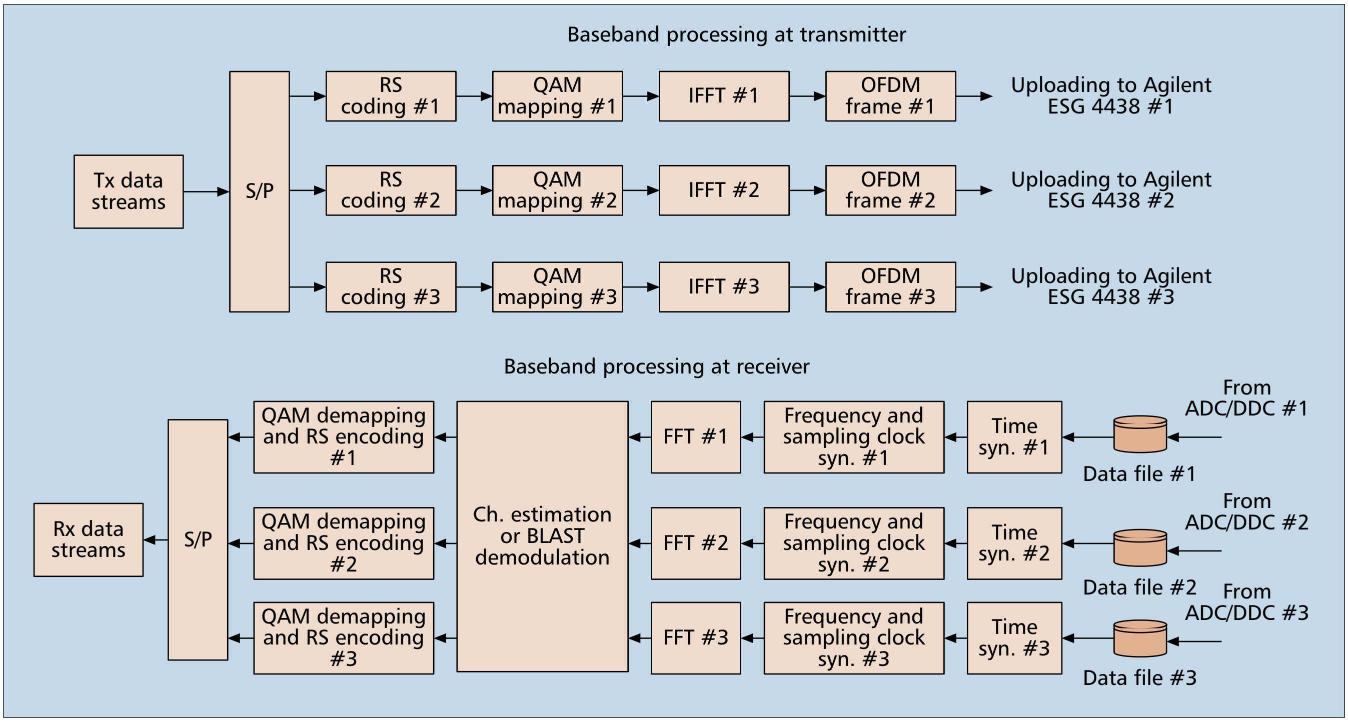

Figure 3. *A block diagram of the baseband processing performed at the transmitter and receiver.*

synchronization, sampling clock synchronization, FFT, and channel estimation.

Time Synchronization

The task of time synchronization is to locate the first sample of an OFDM frame from the received baseband signal. The short preamble given by the IEEE 802.16 standard is inserted at the beginning of the OFDM frame for this purpose. We use a cross-correlator to perform time synchronization since it outputs a correlation curve with unique peaks, which helps to reduce the possibilities of both missed detection and false alarm.

Carrier Frequency Synchronization

A carrier frequency offset is caused by frequency drifts between the LOs at the transmitter and those at the receiver. A Doppler shift can also impact the offset. A frequency offset leads to the loss of orthogonality between the subcarriers and introduces intercarrier interference (ICI). An offset of a fraction of the subcarrier spacing results in the scattering of demodulated QAM constellations, while an offset of an integral multiple of subcarrier spacing results in a cyclic shift of the sequence of demodulated QAM symbols.

A typical carrier frequency offset estimation method compares two consecutive OFDM symbols carrying identical information to extract the phase difference, which is proportional to the carrier frequency offset [8].

Sampling Clock Synchronization

A sampling clock offset reflects the misalignment between the clocks of the digital-to-analog converter (DAC) at the transmitter and the ADC at the receiver. A sampling clock offset causes phase rotations and attenuation of the demodulated QAM symbols as well as ICI. The method of comparing two consecutive OFDM symbols is applied here as well with the additional consideration that the phase difference caused by a sampling clock offset is proportional to the subcarrier index.

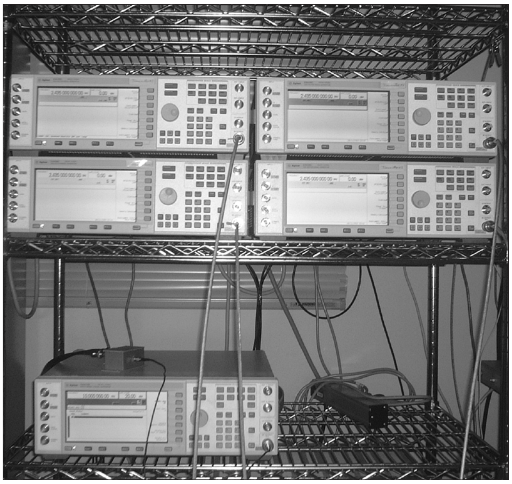

Figure 4. *The transmitter of the 3 × 3 OFDM/BLAST wireless MAN testbed.*

FFT

By using IFFT at the transmitter, an OFDM system effectively creates multiple narrowband flat fading channels, which allows us to employ simple detection techniques to recover the data. In OFDM, the QAM symbols are created in the frequency domain, so FFT is used at the receiver to convert the baseband signal from the time domain to the frequency domain. The channel estimation and BLAST detection are then performed.

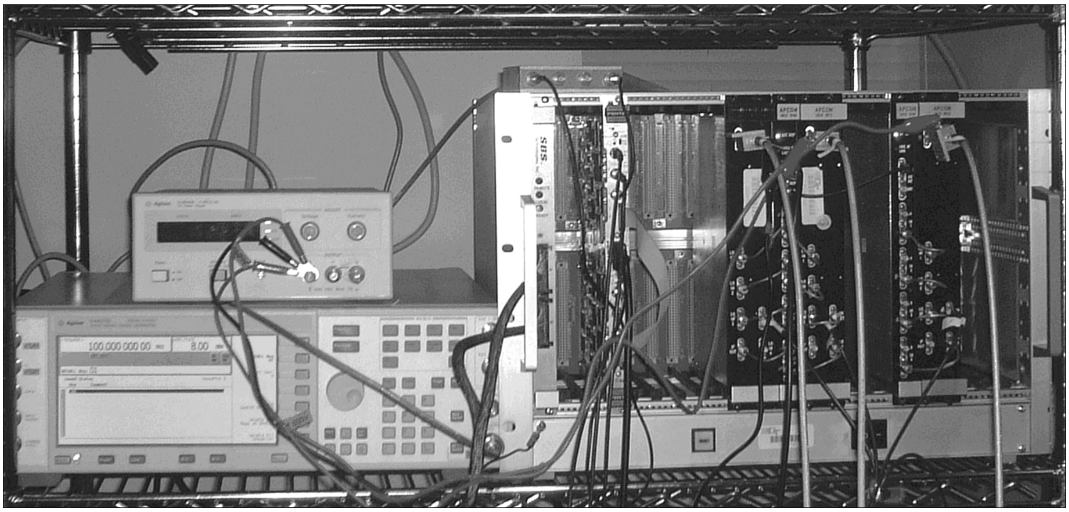

■ **Figure 5.** *The receiver of the 3 × 3 OFDM/BLAST wireless MAN testbed.*

CHANNEL ESTIMATION

Each subcarrier is associated with nine complex channel gains. Because there are 200 subcarriers used to transmit the payload data, the channel gains are expressed as a 3 × 3 × 200 matrix. The BLAST demodulator needs the channel gains in order to recover the transmitted data.

In this system, three OFDM training symbols, located between the short preamble and the payload OFDM symbols, are used to estimate the channel gains. The training symbol is the long preamble given by the IEEE 802.16 standard. Only the odd subcarriers are estimated, and the channel gains of the even subcarriers are obtained by interpolation.

Detector	Divisions	Multiplications	Additions	SQRTs
Linear	13	29	20	0
PDF	17	48	34	0
ODF	25	76	56	2

■ **Table 2.** *Required computations for a 3 × 3 MIMO system.*

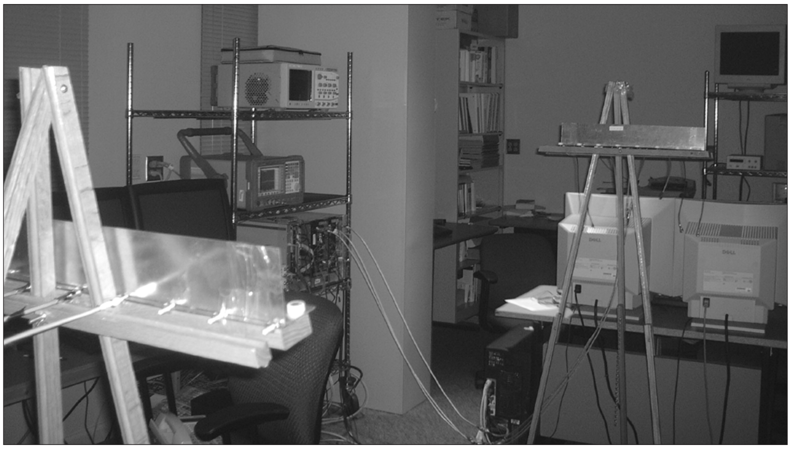

■ **Figure 6.** *The LOS test field in Room 268, GCATT, Georgia Institute of Technology.*

BASEBAND PROCESSING FOR DATA RECOVERY: BLAST DETECTION

After the initial baseband processing, the receiver demodulates the layered QAM symbols and de-maps them to bits. Then, a RS decoder is applied to perform bit error correction. In this section, we frame the detection problem in the context of MIMO channels and evaluate three typical detection strategies.

In designing the BLAST detector, there is a trade-off between performance and complexity. Given a transmitter with N antennas, each transmitting symbols from an alphabet of size Q, finding the correct decision vector can be framed in the context of a Q-ary tree search with N levels. Each node in the tree represents a decision vector and there are a total of Q^N nodes.

The size of this decision tree indicates the complexity of BLAST detection. The complexity is increased by a factor of the number of payload subcarriers. Currently, the detectors are implemented offline without restriction on the computational complexity. However, in order to eventually achieve a real-time detector, only low-complexity detectors are considered. Three such detectors are briefly summarized below, including the linear detector, ordered decision feedback (ODF) detector, and partial decision feedback (PDF) detector.

LINEAR DETECTOR

The linear detector inverts the channel matrix and right-multiplies it by the received vector. This method separates the layered data streams, but also amplifies the Gaussian noise. The output of the multiplication is then sliced to the nearest symbol in the QAM constellation.

The linear detector does not exploit the tree structure. Instead it detects each symbol independently, like N different tree searches of depth 1.

ODF DETECTOR

The ODF detector improves on the performance of the linear detector by using the previous decisions of the detector. It first orders the levels of the tree, then proceeds from the root node to a leaf node by choosing the branch at each level with the smallest mean-squared error (MSE). This is obviously less robust than an exhaustive tree search, but it is also much less complex.

The order in which the symbols are detected is crucial to the performance of the ODF detector. Since all the transmitted symbols arrive at the receiver simultaneously, the receiver may choose to detect them in any order. The ODF detector detects the more reliable symbols first, then removes their contribution from the signal to better mitigate the interference generated by the other symbols. The best symbol ordering is the so-called BLAST ordering, which minimizes the maximum MSE and approximately minimizes the joint error probability of the DF detector [9].

One way to implement the ODF detector involves noise prediction. Like the linear detector, the noise-predictive ODF detector begins by inverting the channel matrix and right-multiplying it by the receive vector. This introduces correlation to the Gaussian noise. Using linear prediction, a prediction filter can be calculated to reduce the noise variance. A computationally efficient algorithm that finds the BLAST detection order and calculates the prediction filter simultaneously was presented in [10].

PDF Detector

The PDF detector is an approximation of the ODF detector. Whereas the ODF detector uses every available decision to help predict the noise, the PDF detector uses only the strongest decision. For the PDF detector, the calculation of the prediction filter is much simpler than that of the ODF detector. Therefore, the complexity and performance of the PDF detector is between that of the ODF and linear detectors. The PDF detector is a means of trading performance for reduced complexity.

The tree search interpretation of the PDF detector is a combination of the linear and ODF tree searches. At the first level, the least expensive branch is chosen and the other $Q - 1$ branches are discarded. The linear detector approach is used to search the remaining subtree.

Table 2 gives the number of computations required by each detection technique to recover the layered data streams on a single subcarrier. The experimental performance is presented next.

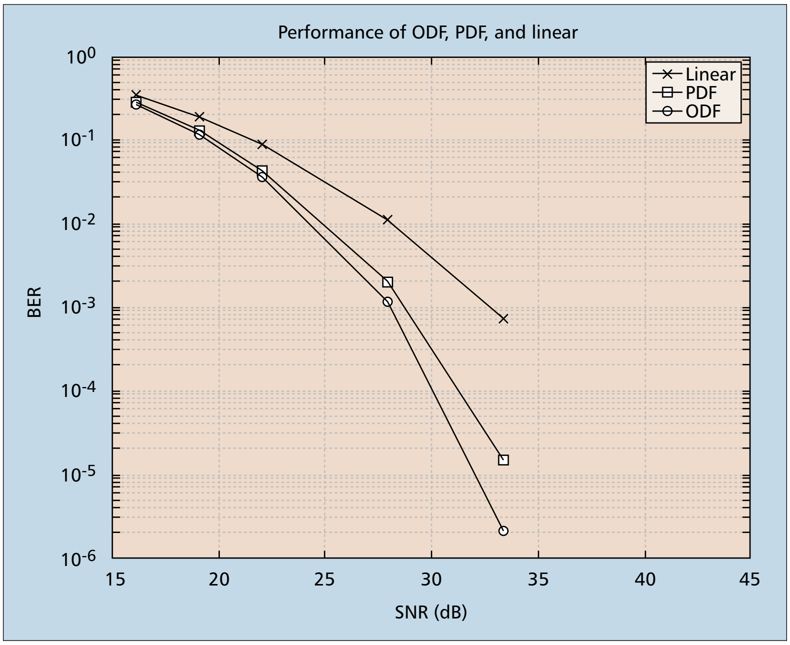

Figure 7. *The performances of the linear, PDF, and ODF in the case of LOS propagation.*

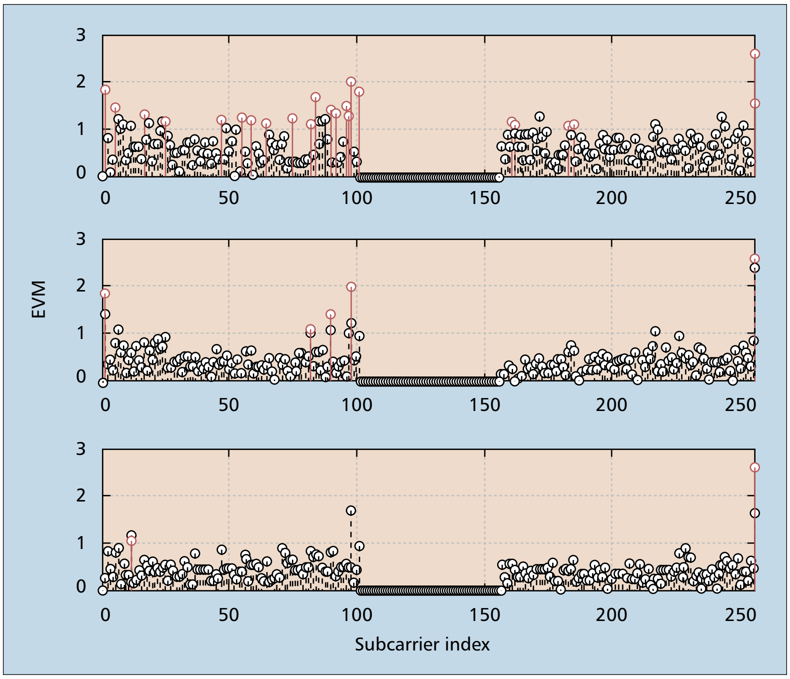

Figure 8. *The distribution of error symbols in three layered OFDM payload symbols where SNR = 36 dB.*

Experimental Results and Analysis

We first explore line-of-sight (LOS) transmission. The experiment was conducted in Room 268 of the Georgia Center for Advanced Telecommunications Technology (GCATT), a laboratory with several metal shelves along the walls and one work desk located in the middle. As shown in Fig. 6, the three transmitters transmit data streams at a power level of 0 dBm over three omnidirectional antennas, spaced by half a wavelength and mounted at a height of 1.5 m above the floor. A similar antenna configuration is used for the receivers, and the distance between the transmitters and receivers is approximately 2 m. The test is performed at a center frequency of 2435 MHz.

Figure 7 compares the performances of the three BLAST detectors without an error correction code. As expected, the ODF detector outperforms the PDF detector, which outperforms the linear detector. The PDF detector performs almost as well as the ODF detector while reducing the calculation load by about 38 percent, referring to Table 2.

In the above BLAST demodulation, the different SNRs are realized by artificially adding additional Gaussian noise to the received baseband signal. The channel gains were verified to be constant during the period of one OFDM frame.

The distribution of the error symbols provides important information for selecting the proper coding scheme. As an example, Fig. 8 shows the error vector magnitude (EVM), which is defined as the Euclidean distance between the demodulated QAM symbol and the transmitted QAM symbol, vs. the subcarrier index for three payload OFDM symbols where SNR = 36 dB. The EVMs shown in red identify the subcarriers with symbol errors. There are 24, five, and two symbol errors for the three OFDM payload symbols, respectively. The fact that one transmitter is less reliable than the others suggests that an interleave should be introduced to scatter symbol errors evenly across the three transmitters.

Having verified the performance of the testbed in a LOS environment, additional experiments were conducted over four non-LOS links. The floorplan is shown in Fig. 9 with the approximate location of the receiver (marked RX in red) and four different locations of the transmitter (marked TX1–TX4). The power transmitted at each of the three antennas is set to 12 dBm for all four scenarios. Figure 10 gives the curves of symbol error rate (SER), defined as the ratio of the number of error symbols and that of the total layered QAM symbols, vs. the SNR for all of the four positions. The SER curves are obtained by using ODF detector without an error correction code.

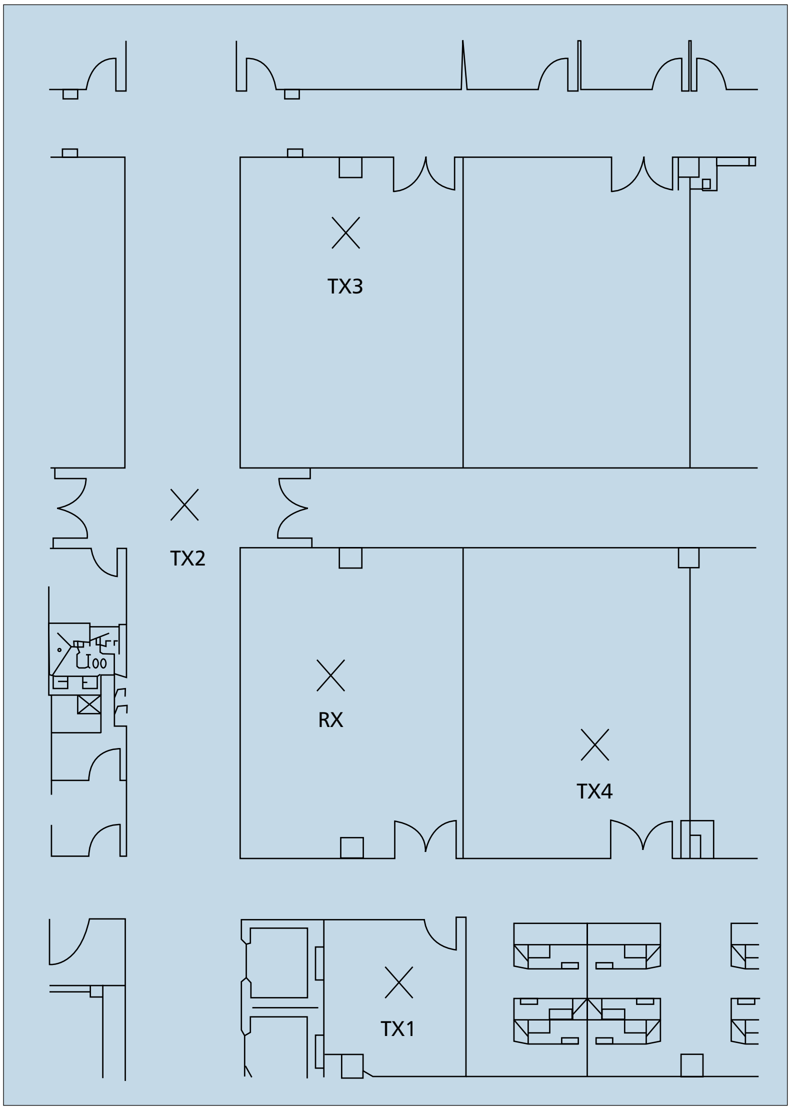

Figure 9. *The floorplan of the test field where the non-LOS measurements were conducted.*

From the experimental results reported in Figs. 7 and 10, we can see that while BLAST systems offer extremely high data rates, they demonstrate mean BER/SER performances even in the cases with SNRs larger than 30 dB. Thus, some powerful coding or/and redundancy transmission schemes should be adopted to enhance the transmission reliability.

Conclusion

The mechanism of parallel transmission unshackles the limitation of the maximum ISI-free data rate over a wireless channel due to multipath fading. OFDM is a frequency domain parallel transmission scheme, while BLAST sends the information in parallel in the space domain. The combination of OFDM and BLAST offers a robust approach to achieve extremely high data rates that cannot be achieved with traditional wireless technologies.

The Georgia Institute of Technology has developed a 3×3 OFDM/BLAST wireless MAN testbed, and some preliminary experimental results are presented in this article. Further experimentations and analyses are in progress.

Acknowledgments

This work was supported in part by a grant from the National Science Foundation and by the Georgia Electronics Design Center project, a Georgia State based research project focused in part on developing technology for next-generation broadband communications.

References

[1] G. D. Golden *et al.*, "Detection Algorithm and Initial Laboratory Results Using V-BLAST Space-time Communication Architecture," *Elect. Lett.*, vol. 35, Jan. 1999, pp. 14–15.

[2] IEEE P802.16a/D4-2002, "Part 16: Air Interface for Fixed Broadband Wireless Access Systems."

[3] M. Sellathurai and S. Haykin, "T-BLAST for Wireless Communications: First Experimental Results," *IEEE Trans. Vehic. Tech.*, vol. 52, May 2003, pp. 530–35.

[4] H. Sampath *et al.*, "A Fourth-generation MIMO-OFDM Broadband Wireless System: Design, Performance, and Field Trial Results," *IEEE Commun. Mag.*, vol. 40, no. 9, Sept. 2002, pp. 143–49.

[5] R. J. Piechocki *et al.*, "Performance Evaluation of BLAST-OFDM Enhanced Hiperlan/2 using Simulated and Measured Channel Data," *Elect. Lett.*, vol. 37, no. 18, 30 Aug. 2001, pp. 1137–39.

[6] M.D. Batariere *et al.*, "An Experimental OFDM System for Broadband Mobile Communications," *Proc. IEEE VTC 2001-Fall*, vol. 4, pp. 1947–51.

[7] W. Xiang, T. Pratt, and X. Wang, " A Software Radio Testbed for Two-transmitter Two-receiver Space-time Coding OFDM wireless LAN," *IEEE Commun. Mag.*, vol. 42, no. 6, June 2004, pp. S20–S28.

[8] P. Moose, "A Technnique for Orthogonal Frequency-division Multiplexing Frequency Offset Correction," *IEEE Trans. Commun.*, vol. 42, Oct. 1994, pp. 2908–14.

[9] G. J. Foschini *et al.*, "Simplified Processing for Wireless Communication at High Spectral Efficiency," *IEEE JSAC*, vol. 17, 1999, pp. 1841–53.

[10] D. W. Waters and J. R. Barry, "Noise-Predictive Decision-Feedback Detection for Multiple-Input Multiple-Output Channels," *IEEE Int'l. Symp. Advances in Wireless Commun.*, invited paper, MA 1.4, Sept. 2002.

Additional Reading

[1] G. J. Foschini, "Layered Space-Time Architecture for Wireless Communication in a Fading Environment When Using Multiple Antennas," *Bell Labs. Tech. J.*, vol. 1, no. 2, Autumn 1996, pp. 41–59.

Biographies

Weidong Xiang [M] (xwd@umich.edu) received his M.S.E.E. and Ph.D. degrees from Tsinghua University, Beijing, China, in 1996 and 1999, respectively. From 1999 to 2004 he worked as a post-doctoral fellow and then research scientist in the Software Radio Laboratory (SRL) at Georgia Institute of Technology, Atlanta. In September 2004 he joined the ECE Department, University of Michigan-Dearborn as an assistant professor. His research interests include MIMO, OFDM, wireless LAN/MAN, 3G/4G cellular systems, software radio, and smart antenna.

Deric W. Waters (StM) received B.S. degrees in electrical engineering and computer science from Texas Tech University in 1999. From 2000 to 2002 he studied at Georgia Tech Lorraine, Metz, France, and l'Ecole Supérieure d'Ingénieurs de Marseille, France, while earning an M.S. degree in electrical and computer engineering from Georgia Institute of Technology. Since 2002 he has been pursuing a Ph.D. degree in electrical and computer engineering from Georgia Institute of Technology in the area of signal processing for communication systems.

Thomas Pratt [M] received a B.S. degree from the University of Notre Dame, Indiana, in 1985, and M.S. and Ph.D. degrees in electrical engineering from Georgia Institute of Technology in 1989 and 1999, respectively. He heads the software radio laboratory at Georgia Tech, where research has focused principally on MIMO-OFDM, space-time adaptive processing, WLAN coexistence and interference suppression, multiple-antenna architectures for MIMO and array processing, signal processing for GSM systems, spread spectrum waveform development, channel modeling, and mobile communications. He is a principal research engineer at the Georgia Tech Research Institute.

John R. Barry [M] received a B.S. degree in electrical engineering from the State University of New York, Buffalo, in 1986, and M.S. and Ph.D. degrees in electrical engineering from the University of California, Berkeley, in 1987 and 1992, respectively. Since 1992 he has been with Georgia Institute of Technology, where he is an associate professor with the School of Electrical and Computer Engineering. His research interests include wireless communications, equalization, and multiuser communications. He is a coauthor with E. A. Lee and D. G. Messerschmitt of *Digital Communications*, third edition (Norwell, MA: Kluwer, 2004), and the author of *Wireless Infrared Communications* (Norwell, MA: Kluwer, 1994).

Brett T. Walkenhorst received B.S. and M.S. degrees in electrical engineering from Brigham Young University, Provo, Utah, in 2001. From 2001 to 200 he worked as a design engineer at Lucent Technologies, Bell Laboratories, Denver, Colorado. He is currently a research engineer at Georgia Tech Research Institute, Atlanta. His research interests include MIMO wireless communications, channel estimation and tracking, and neural networks.

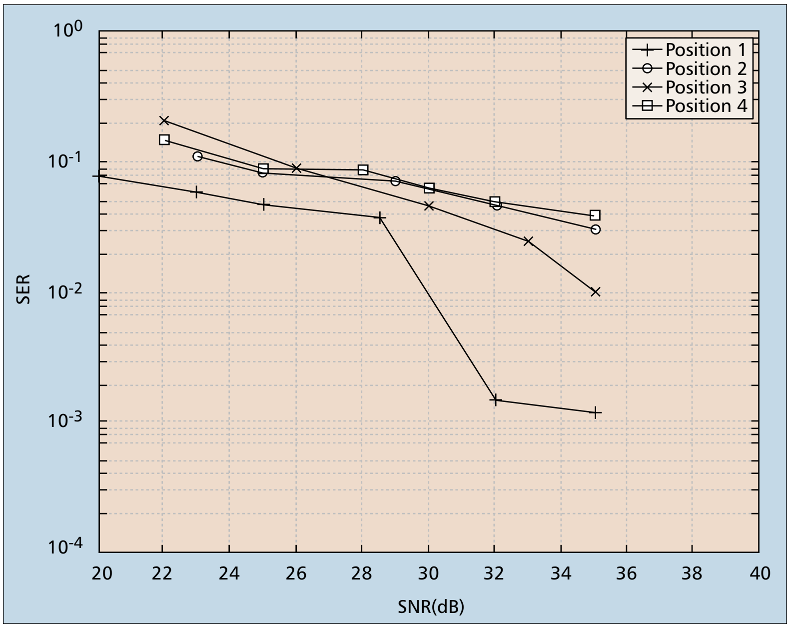

Figure 10. *The SER vs. SNR curves in the four non-LOS wireless links shown in Fig. 9.*